How to cite: *Angew. Chem. Int. Ed.* **2021**, *60*, 11262–11266
International Edition: doi.org/10.1002/anie.202102160
German Edition: doi.org/10.1002/ange.202102160

Supramolecular Chemistry | Hot Paper

Dynamic Protease Activation on a Multimeric Synthetic Protein Scaffold via Adaptable DNA-Based Recruitment Domains

*Tsuyoshi Mashima, Bas J. H. M. Rosier, Koji Oohora, Tom F. A. de Greef, Takashi Hayashi, and Luc Brunsveld**

Abstract: *Hexameric hemoprotein (HTHP) is employed as a scaffold protein for the supramolecular assembly and activation of the apoptotic signalling enzyme caspase-9, using short DNA elements as modular recruitment domains. Caspase-9 assembly and activation on the HTHP platform due to enhanced proximity is followed by combinatorial inhibition at high scaffold concentrations. The DNA recruitment domains allow for reversible switching of the caspase-9 assembly and activity state using short modulatory DNA strands. Tuning of the recruitment domain affinity allows for generating kinetically trapped active enzyme complexes, as well as for dynamic repositioning of caspases over scaffold populations and inhibition using monovalent sink platforms. The conceptual combination of a highly structured multivalent protein platform with modular DNA recruitment domains provides emergent biomimicry properties with advanced levels of control over protein assembly.*

Spatial and temporal organization of proteins represents an important principle for controlling signalling pathway response and regulating downstream intracellular events in biological signalling processes.[1] Scaffold proteins play a pivotal role in providing stable, but frequently adaptive, organization platforms for the assembly of multiple proteins and resulting enzyme activation.[2,3] Proximity-induced protein–protein interactions are key regulation events to enable robust switching of enzyme activity.[4,5] The construction of synthetic platforms for protein assembly and enzyme activation provides entries to revealing the molecular mechanisms behind spatial organization in signalling pathways[6] and a compact set of diverse scaffolds have shown great promise, including synthetic materials,[7,8] DNA origami,[9,10] and protein scaffolds.[11,12] Several proteins have been shown to be appropriate engineering scaffolds for assembling and activating enzymes,[6,13,14] but often harbor limitations with regard to possibilities for tuning of the affinities of the recruitment domains.

Caspases are an essential class of enzymes controlling apoptosis by an archetypical proximity-induced activation mechanism,[4] exemplified by caspase-8 activation on a supramolecular organizing center at the membrane[15] and caspase-9 activation on the apoptosome (Figure 1b).[16,17] In case of the latter, caspase-9 assembles on the ring-shaped heptameric apoptosome by binding to the caspase recruitment domains (CARDs) located in the center of the platform.[18] Recent studies suggest that caspase-9 activation is triggered by proximity-induced dimerization and that the proteolytic cleavage results in dynamic protease activity.[14–19] Although the molecular structure of the apoptosome is known,[20] studying the molecular principles behind enzymatic activation is challenging due to the complex multi-component structures involved and limited flexibility to control caspase-9 recruitment in terms of numbers and affinity of the recruitment domain.

Here, we demonstrate the conceptual approach to use short DNA elements[21] as programmable and flexible recruitment domains for modular and dynamic protein assembly on a well-structured multimeric protein scaffold, as illustrated via caspase-9 assembly and activation (Figure 1c). Such a hybrid approach allows the evaluation of the principles behind enzyme assembly onto protein-based scaffolds like those found in most cellular processes, while ensuring in vitro control over the recruiting properties using programmable DNA recognition elements. The symmetric, rigid, and thermostable hexameric tyrosine-coordinated heme protein (HTHP, Figure 1a)[22] was employed as a scaffolding platform displaying the DNA recruitment domains to assemble caspase-9 proteins. The symmetric, multimeric structure and size of HTHP resembles the structure of various scaffold proteins and organizing centers in the cell,[2,23] and therefore represents a good candidate to illustrate our strategy. We show that the DNA elements act as efficient caspase-9 recruitment

[*] Dr. T. Mashima, Dr. B. J. H. M. Rosier, Prof. Dr. T. F. A. de Greef, Prof. Dr. L. Brunsveld
Institute for Complex Molecular Systems and
Laboratory of Chemical Biology
Department of Biomedical Engineering
Eindhoven University of Technology
P.O. Box 513, 5600 MB Eindhoven (The Netherlands)
E-mail: l.brunsveld@tue.nl
Dr. K. Oohora, Prof. Dr. T. Hayashi
Department of Applied Chemistry
Graduate School of Engineering
Osaka University
Suita 565–0871, Osaka (Japan)
Prof. Dr. T. F. A. de Greef
Computational Biology group
Department of Biomedical Engineering
Eindhoven University of Technology
Eindhoven (The Netherlands)
Supporting information and the ORCID identification numbers for the authors of this article can be found under: https://doi.org/10.1002/anie.202102160.

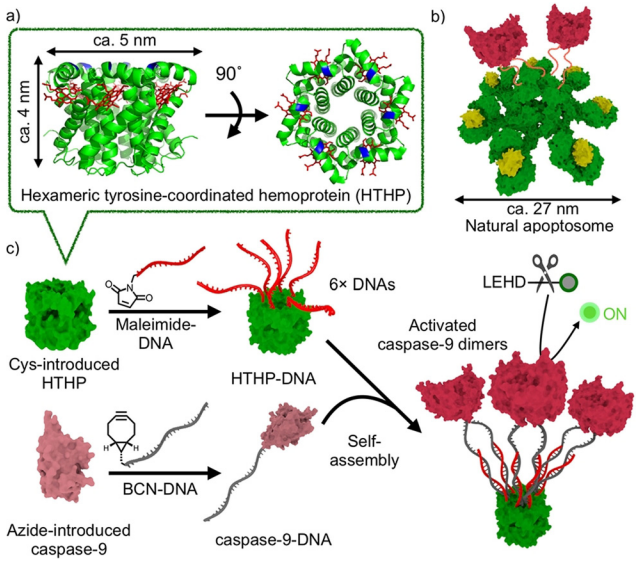

Figure 1. Caspase-9 assembly on HTHP via DNA recruitment domains. a) Crystal structure of HTHP (PDB ID; 2OYY). Heme groups are indicated in red (stick representation). The cysteine mutations at position 44 for DNA conjugation are indicated in blue. b) Structure of the apoptosome (green) that activates tethered caspase-9 via proximity-induced dimerization. Cytochrome *c* is indicated in yellow. c) Schematic overview of the synthesis and platform assembly strategies. HTHP is functionalized with 12–15-nt DNAs via maleimide coupling at Cys-44. Caspase-9 monomer (light red) is labeled with a complementary DNA using strain-promoted azide–alkyne cycloaddition. Proximity-induced activity of caspase-9 dimers (deep red) is monitored using the Ac-LEHD-AFC substrate.

domains and that, depending on the strength of the DNA hybridization, stably trapped assemblies are formed or dynamic exchange between the platforms takes place, with concomitant modulation of the enzymatic activity. Additionally, the DNA elements allow for reversible on–off switching via modulation of the recruitment of caspase-9 to the HTHP protein platform.

Site-specific conjugation of HTHP to single-stranded DNAs was performed using thiol–maleimide coupling (Figure 1c) to a single cysteine residue introduced into each monomer unit of wildtype HTHP by site-directed mutagenesis (see Supporting Information). The V44 residue was selected as the mutation site, being located on the top face of the hexamer with an approximately 3 nm distance between adjacent V44 residues. The HTHP cysteine mutant ($HTHP^{V44C}$) was expressed in *E. coli* and purified by anion exchange and size exclusion chromatography (SEC).[24] Because of the strong intermolecular interactions between HTHP monomers, the protein is always obtained in its stable hexameric form.[22] After reaction, the HTHP–DNA bioconjugates were purified using SEC, and characterized by SDS-PAGE and analytical SEC (Figure S1 and S3). The conjugation efficiency of both the 15-nucleotide (15-nt) and 12-nt long ssDNA strands to $HTHP^{V44C}$ (affording HTHP–DNA15 and HTHP–DNA12, respectively) was >95% (Figure S1). This thus delivers HTHP platforms containing 6 DNA-based protein recruitment domains. DNA-conjugated caspase-9 enzyme, caspase-9–DNA, was obtained using strain-promoted azide–alkyne cycloaddition to azide-functionalized caspase-9, as described previously.[25]

The caspase-9 activities at different platform compositions and over time were evaluated using the synthetic fluorogenic substrate Ac-LEHD-AFC[26] that becomes fluorescent upon cleavage by activated caspase-9. The enzymatic activity of the caspase-9–DNA conjugate (24 nM) increased 5-fold upon the presence of a stoichiometric amount of DNA-functionalized HTHP platform (HTHP–DNA15, 4 nM, HTHP concentration was calculated as hexamer; Figure 2a,b). This activity enhancement is in the same range as seen in previous works, which used DNA origami and supramolecular wire platforms.[8,25] No increase in caspase-9 activity was observed when non-DNA-functionalized HTHP ($HTHP^{WT}$, 4 nM) was added or when HTHP–DNA15 with mismatched DNA strands was added (Figure S4). These findings indicate that the platform without valid recruitment domains does not influence the enzymatic activity of caspase-9. Together, this shows that the DNA-functionalized caspase-9 becomes active upon recruitment by the DNA-functionalized HTHP platform.

Next, we varied the HTHP platform concentration and observed a bell-shaped activity profile with maximal enzymatic activity between 1–2 equivalents of the DNA recruitment domains on the HTHP platform (Figure 2c). This suggests that the enzymatic activity for the fully occupied platform (at 1 equivalent of recruitment domains) is comparable to the activity achieved when there is an up to 2-fold amount of the platform (Figure 2c, right graph). In the latter case, on average only half of the binding sites would be occupied in case of a statistical distribution. A further increase in the HTHP platform concentration led to a notable decrease in the enzymatic activity, most probably due to dispersion of enzyme monomers over the excess scaffolds. This combinatorial inhibition decreases the fraction of platforms containing active caspase-9 dimers, leading to a decrease in activity.[27–29] The relatively high activity at the larger scaffold excesses is most probably related to the intrinsic affinity between caspase-9 monomers and the cooperative formation of the ternary complex between HTHP and caspase-9 dimers.[13,25]

The high DNA hybridization affinity on the HTHP–DNA15 platform would prevent subsequent reversible exchange from the DNA recruitment domains and between the platforms (Figure S5). In order to study such exchange behavior, also the HTHP–DNA12 platform was prepared, which is based on the shorter and weaker binding 12-nt DNA recruitment domain (Figure 2d,e). The basal activity of caspase-9 assembled on the HTHP–DNA12 platform is similar to that of the HTHP–DNA15 platform (Figure 2f). Interestingly, the HTHP–DNA12 platform indeed showed reversible recruitment. The activity of an equimolar mixture of caspase-9–DNA conjugate with the HTHP–DNA12 platform decreased upon addition of an additional amount of the HTHP–DNA12 platform, indicative for a re-equilibration event of the caspase-9 population over the HTHP platforms (Figure S6). This is in contrast to the behavior of the HTHP–DNA15 platform and testifies to the modularity of the DNA

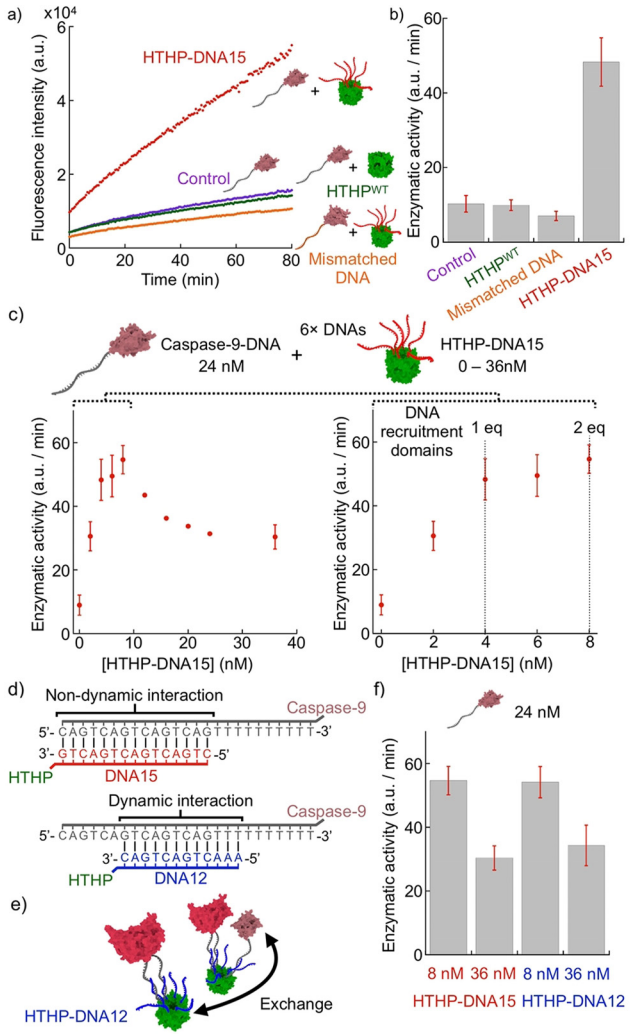

Figure 2. Caspase-9 activation by DNA-mediated recruitment to the HTHP platform. a) Representative kinetic time traces and b) overall enzymatic activity of caspase-9 (24 nM) upon assembly on HTHP using 15-nt DNA hybridization (4 nM, HTHP–DNA15, red). Each HTHP platform carries 6 DNA15 recruitment domains. Background activity of caspase-9–DNA alone (green), with HTHP with mismatched DNA elements (4 nM, orange), and in presence of wildtype HTHP (4 nM, blue). Enzymatic activity was determined from the slope of the fluorescence curves between the first 40 to 80 minutes. c) Effect of HTHP–DNA15 platform concentration on the enzymatic activity of caspase-9. Equivalents indicate the concentration of individual HTHP proteins. The right graph shows an expanded section at low platform concentrations between 0 and 2/6 equiv HTHP–DNA15. d) DNA sequences of the caspase-9-DNA conjugate (gray), HTHP–DNA15 (red) and HTHP–DNA12 (blue). e) Schematic representation of dynamic exchange between platforms by use of 12-bp hybridization on HTHP–DNA12. f) Comparison of the enzymatic activity of caspase-9 tethered to either HTHP–DNA15 or HTHP–DNA12. All measurements were performed in triplicate with error bars representing the standard deviation, and the total caspase-9-DNA concentration at 24 nM.

recruitment domains to enable addressing different kinetic regimes in protein assembly and sorting.

Complex behavior depends on temporal control over molecular processes and higher-order response dynamics through for example, feedback loops and amplification. En route to such systems, stimuli-responsiveness was introduced into the HTHP-based platform by addition of DNA control elements. Such DNA molecular stimuli, analogous to small molecules or protein effectors typically used by nature,[30,31] can either interact with the HTHP platform or with the capase-9 building blocks and therewith block or enable enzyme recruitment and activation. First, we used a blocker strand (blocker1) that suppresses enzyme activity by binding strongly to the DNA recruitment domains on the HTHP platform and that subsequently can be removed by a displacer strand (displacer1) using toehold-mediated strand displacement (Figure 3a and S7). The HTHP–DNA15 platform was temporarily inhibited by the blocker1 and upon addition of the displacer1, the enzyme activity sharply increased (Figure 3b). The temporally controlled release of the blocker strand thus enables the recruitment and activation of caspase-9 on the HTHP scaffold.

In a second system, we adapted the design of the blocker–displacer system to allow multiple cycles of induction and

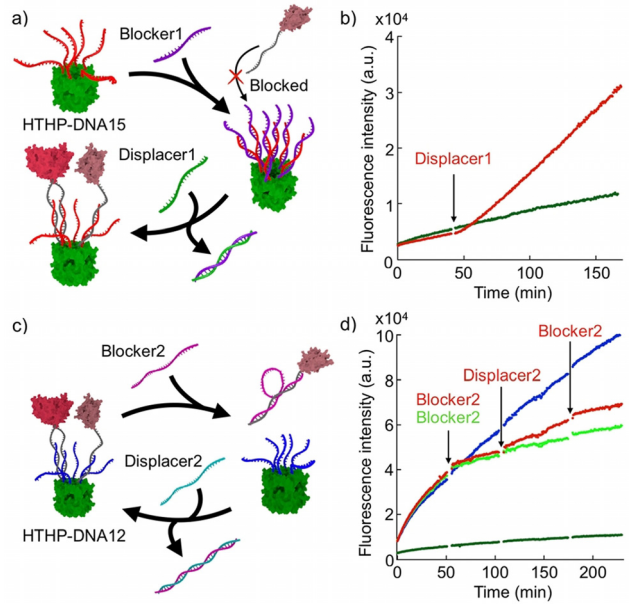

Figure 3. DNA-based control elements enable selective switching of enzymatic activity. a) Schematic representation of the initiation of enzymatic activity by displacement of blocker strands (purple) from the protein binding strands (red) on HTHP using a displacer strand (green). See Figure S7 for details regarding the sequence design of the DNA elements. b) Kinetic traces of caspase-9 enzyme activity. Platforms were assembled at 8 nM using HTHP–DNA15 and combined with 24 nM caspase-9–DNA conjugate and 28 nM blocker strand. After 40 min, either 32 nM (red) or 0 nM (green) of the displacer strand was added. c) Schematic representation of the reversible switching of tethered enzyme activity using blocker–displacer strand cycles (indicated in pink and cyan, respectively). See Figure S8 for details regarding the sequence design of the DNA elements. d) Kinetic traces of caspase-9 enzyme activity. Platforms were assembled at 8 nM using HTHP–DNA12 and combined with 24 nM caspase-9-DNA. At various time points indicated by arrows, displacer and blocker strands were added. For the red curve, 28 nM blocker, 28 nM displacer, and 32 nM blocker were added at 60, 120, and 180 min, respectively. For the light green curve, only 28 nM blocker were added at 60 min. A positive control without addition of blocker or displacer is indicated in blue, while background activity of caspase-9-DNA conjugate without HTHP is indicated in dark green.

inhibition of enzymatic activity, using the reversible DNA hybridization on the more transient binding HTHP–DNA12 platform (Figure 3c and S8 for design). Starting with caspase-9 recruited and activated on the platform, the addition of a blocker strand (blocker2) that binds to the caspase-9–DNA conjugate resulted in a decrease in enzyme activity (Figure 3d). The enzyme activity could be reversibly restored upon addition of a displacer strand (displacer2) that binds and sequesters the blocker, priming caspase-9 for reactivation on the HTHP platform (Figure 3d and S8). Full restoration of enzymatic activity compared to the control was not observed (compare red and blue curves, Figure 3d) and can be explained by a combination of effects including incomplete sequestration of the blocker and kinetics of the displacement reaction. Nevertheless, a second addition of the blocker2 allowed again to decrease the enzymatic activity (Figure 3d). Taken together, these results indicate that the HTHP platforms with DNA recruitment domains can be designed to respond to external stimuli that influence the assembly behavior and activity of the tethered enzymes.

The HTHP–DNA12 and HTHP–DNA15 scaffolds allow for the study of the effects of dispersion of the caspase-9 enzymes over two scaffolds with different recruitment domain affinities, where one of the two scaffolds can behave as an inhibitory sink.[32] To generate such a sink scaffold, we prepared a monofunctionalized HTHP platform that only contains a single DNA15 recruitment domain on which proximity-induced dimerization of caspase-9 monomers cannot occur. This variant (HTHP–monoDNA15) was synthesized by reacting an excess of HTHP^{V44C} with maleimide-functionalized 15-nt DNA. The reaction mixture was first purified with SEC to remove unreacted DNA, followed by anion exchange chromatography to remove unreacted HTHP and HTHP containing more than one DNA strand (Figure S9). The caspase-9 activity was first evaluated in the presence of various concentrations of monovalent platform HTHP–monoDNA15 (Figure 4a). Indeed, the addition of HTHP–monoDNA15 did not result in enzyme activation. At platform concentrations exceeding 0.5 equiv, even a slight decrease in enzymatic activity could be observed (Figure 4b), suggesting that tethering of a single caspase-9 monomer to the platform actually inhibits background enzymatic and caspase-9 dimerization activity. This could result from a weakening of the caspase-9 dimerization in solution[33] by the attachment of the bulky HTHP platform.

The monovalent, inactivating HTHP–monoDNA15 platform was then used to sequester caspase-9 monomers away from an activating HTHP platform, effectively shifting the equilibrium from a high-activity to a low-activity state. To this end, a 2-times excess of HTHP–monoDNA15 was added to caspase-9 assembled on either the HTHP–DNA15 or the HTHP–DNA12 platform (Figure 4c). The caspase-9 activity on the HTHP–DNA15 platform with the strongly binding, non-reversible, DNA recruitment domains was not affected by the addition of the monovalent platform (red curve, Figure 4c). The caspase-9 proteins are thus kinetically trapped on the HTHP–DNA15 platform, ensuring continued activation, despite the presence of platform sinks with free recruitment domains. In contrast, the activity of caspase-9

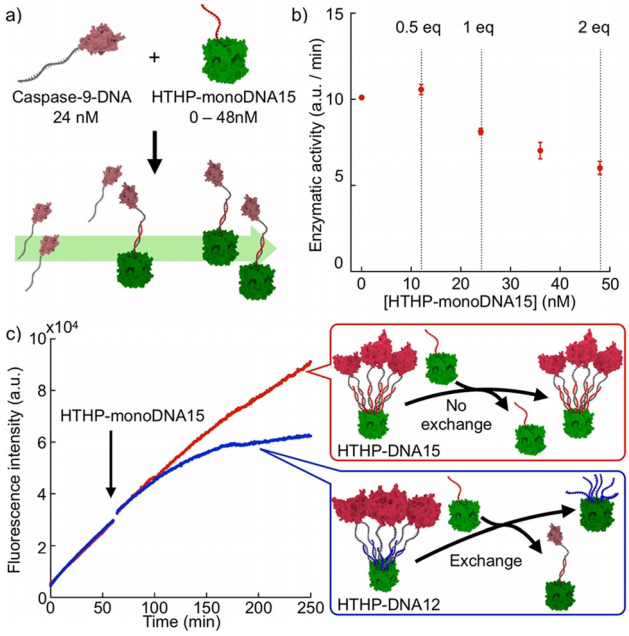

Figure 4. Dynamic enzyme exchange between HTHP platforms results in modulation of activity. a) Schematic representation of the assembly of caspase-9 on a mono-functionalized HTHP–DNA platform. b) Enzymatic activity of caspase-9 (24 nM) combined with varying concentrations of HTHP–monoDNA15. The error bars represent the standard deviation of the measurements performed in triplicate. c) Caspase-9 exchange between HTHP platforms with 6 and 1 recruitment domains, controlled by the interaction strength of the DNA domains. Caspase-9-DNA conjugates were assembled with 8 nM HTHP–DNA15 (red) or HTHP–DNA12 (blue). After 60 min, 48 nM of mono-functionalized HTHP was added to both samples.

assembled on the HTHP–DNA12 platform gradually diminished to background levels in a time period of approximately 100 min. upon addition of the monovalent platform (blue curve). The HTHP–DNA12 platform thus allows for dynamic enzyme exchange to the HTHP–monoDNA15 platform, which reduces the number of activated caspase-9 species, suppressing enzymatic activity. A control experiment using a simple ssDNA strand as inhibitory sink also showed decreasing enzymatic activity over a 100 min time period, albeit with a faster onset most likely caused by the difference in molecular size between the two sinks (Figure S10). Collectively, these results demonstrate that the interplay between the number of enzyme binding sites on the HTHP platform and the interaction strength of the DNA-based recruitment elements enables control over the behavior of tethered caspase-9 enzymes.

This study has highlighted the potential of combining protein-based scaffolds with DNA-based recruitment elements for the generation and study of higher-ordered enzyme assemblies. The combination of a highly structured HTHP protein platform with short, adaptable DNA sequences leads to an advanced level of biomimicry with great modular control.[34] Via the protein platform the number and structural organization of the recruited proteins can be controlled and DNA recruitment domains allow tuning of affinity and dynamics. The presented system and general concept are

expected to enable diverse bottom-up approaches for protein assembly and control of enzyme activation. The combination with protein scaffolds also brings DNA nanotechnology a step closer to applications in cells or in vivo, compared to systems which only consist of DNA.

Acknowledgements

This research was funded by The Netherlands Organization for Scientific Research (NWO) through Gravity Program 024.001.035 and VICI Grant 016.150.366. T.H. acknowledges supports from JSPS KAKENHI JP15H05804, JP15K21707 and JP20H00403.

Conflict of interest

The authors declare no conflict of interest.

Keywords: artificial apoptosome · DNA nanotechnology · enzymes · self-assembly · supramolecular chemistry

[1] R. P. Bhattacharyya, A. Reményi, B. J. Yeh, W. A. Lim, *Annu. Rev. Biochem.* **2006**, *75*, 655 – 680.
[2] M. C. Good, J. G. Zalatan, W. A. Lim, *Science* **2011**, *332*, 680 – 686.
[3] A. S. Shaw, E. L. Filbert, *Nat. Rev. Immunol.* **2009**, *9*, 47 – 56.
[4] S. J. Riedl, Y. Shi, *Nat. Rev. Mol. Cell Biol.* **2004**, *5*, 897 – 907.
[5] V. Csizmok, A. V. Follis, R. W. Kriwacki, J. D. Forman-Kay, *Chem. Rev.* **2016**, *116*, 6424 – 6462.
[6] O. Idan, H. Hess, *Curr. Opin. Biotechnol.* **2013**, *24*, 606 – 611.
[7] F. Jia, B. Narasimhan, S. Mallapragada, *Biotechnol. Bioeng.* **2014**, *111*, 209 – 222.
[8] E. Magdalena Estirado, B. J. H. M. Rosier, T. F. A. de Greef, L. Brunsveld, *Chem. Commun.* **2020**, *56*, 5747 – 5750.
[9] W. Engelen, B. M. G. Janssen, M. Merkx, *Chem. Commun.* **2016**, *52*, 3598 – 3610.
[10] N. Stephanopoulos, *Chem* **2020**, *6*, 364 – 405.
[11] R. J. Conrado, J. D. Varner, M. P. DeLisa, *Curr. Opin. Biotechnol.* **2008**, *19*, 492 – 499.
[12] M. J. Lee, J. Mantell, L. Hodgson, D. Alibhai, J. M. Fletcher, I. R. Brown, S. Frank, W. F. Xue, P. Verkade, D. N. Woolfson, *Nat. Chem. Biol.* **2018**, *14*, 142 – 147.
[13] A. den Hamer, L. J. M. Lemmens, M. A. D. Nijenhuis, C. Ottmann, M. Merkx, T. F. A. de Greef, L. Brunsveld, *ChemBioChem* **2017**, *18*, 331 – 335.
[14] Q. Hu, D. Wu, W. Chen, Z. Yan, C. Yan, T. He, Q. Liang, Y. Shi, *Proc. Natl. Acad. Sci. USA* **2014**, *111*, 16254 – 16261.
[15] M. E. Peter, P. H. Krammer, *Cell Death Differ.* **2003**, *10*, 26 – 35.
[16] P. Li, D. Nijhawan, I. Budihardjo, S. M. Srinivasula, M. Ahmad, E. S. Alnemri, X. Wang, *Cell* **1997**, *91*, 479 – 489.
[17] D. Acehan, X. Jiang, D. G. Morgan, J. E. Heuser, X. Wang, C. W. Akey, *Mol. Cell* **2002**, *9*, 423 – 432.
[18] T. C. Cheng, C. Hong, I. V. Akey, S. Yuan, C. W. Akey, *eLife* **2016**, *5*, 17755.
[19] C.-C. Wu, S. Lee, S. Malladi, M.-D. Chen, N. J. Mastrandrea, Z. Zhang, S. B. Bratton, *Nat. Commun.* **2016**, *7*, 13565.
[20] Y. Li, M. Zhou, Q. Hu, X. C. Bai, W. Huang, S. H. W. Scheres, Y. Shi, *Proc. Natl. Acad. Sci. USA* **2017**, *114*, 1542 – 1547.
[21] M. Madsen, K. V. Gothelf, *Chem. Rev.* **2019**, *119*, 6384 – 6458.
[22] J. H. Jeoung, D. A. Pippig, B. M. Martins, N. Wagener, H. Dobbek, *J. Mol. Biol.* **2007**, *368*, 1122 – 1131.
[23] J. C. Kagan, V. G. Magupalli, H. Wu, *Nat. Rev. Immunol.* **2014**, *14*, 821 – 826.
[24] K. Oohora, S. Hirayama, T. Mashima, T. Hayashi, *J. Porphyrins Phthalocyanines* **2020**, *24*, 259 – 267.
[25] B. J. H. M. Rosier, A. J. Markvoort, B. Gumí Audenis, J. A. L. Roodhuizen, A. den Hamer, L. Brunsveld, T. F. A. de Greef, *Nat. Catal.* **2020**, *3*, 295 – 306.
[26] Q. Yin, H. H. Park, J. Y. Chung, S.-C. Lin, Y.-C. Lo, L. S. da Graca, X. Jiang, H. Wu, *Mol. Cell* **2006**, *22*, 259 – 268.
[27] A. Levchenko, J. Bruck, P. W. Sternberg, *Proc. Natl. Acad. Sci. USA* **2000**, *97*, 5818 – 5823.
[28] J. J. McCann, U. B. Choi, M. E. Bowen, *Structure* **2014**, *22*, 1458 – 1466.
[29] L. J. M. Lemmens, J. A. L. Roodhuizen, T. F. A. de Greef, A. J. Markvoort, L. Brunsveld, *Angew. Chem. Int. Ed.* **2020**, *59*, 12113 – 12121; *Angew. Chem.* **2020**, *132*, 12211 – 12219.
[30] J. A. Zorn, J. A. Wells, *Nat. Chem. Biol.* **2010**, *6*, 179 – 188.
[31] L. Kovbasyuk, R. Krämer, *Chem. Rev.* **2004**, *104*, 3161 – 3187.
[32] D. Meiri, C. B. Marshall, M. A. Greeve, B. Kim, M. Balan, F. Suarez, C. Wu, J. LaRose, N. Fine, M. Ikura, *Mol. Cell* **2012**, *45*, 642 – 655.
[33] M. Renatus, H. R. Stennicke, F. L. Scott, R. C. Liddington, G. S. Salvesen, *Proc. Natl. Acad. Sci. USA* **2001**, *98*, 14250 – 14255.
[34] N. Hannewald, P. Winterwerber, S. Zechel, D. Y. W. Ng, M. D. Hager, T. Weil, U. S. Schubert, *Angew. Chem. Int. Ed.* **2020**, *59*, 6218 – 6229; *Angew. Chem.* **2020**, *132*, 6282 – 6294.

Manuscript received: February 10, 2021
Accepted manuscript online: March 16, 2021
Version of record online: April 8, 2021

